

# Nuclear magnetic transitions in the relativistic energy density functional approach

***N. Paar***

***Department of Physics***

***Faculty of Science, University of Zagreb, Croatia***

Collaborators:

G. Kružić (Univ. of Zagreb & Ericsson-Nikola Tesla), T. Oishi (Univ. of Zagreb)



# NUCLEAR ENERGY DENSITY FUNCTIONALS

- **Nuclear energy density functional (EDF)**

unified approach to describe at the quantitative level nuclear properties across the nuclide map including exotic nuclei – astrophysically relevant properties

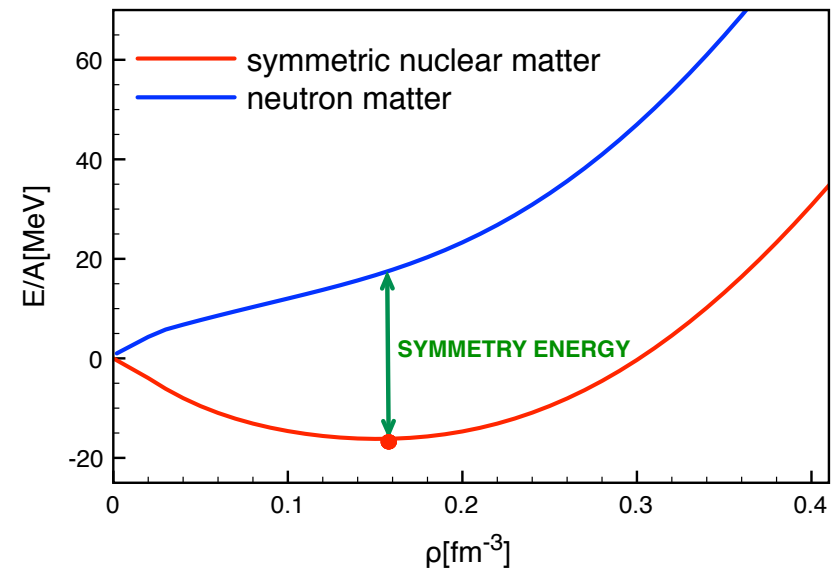
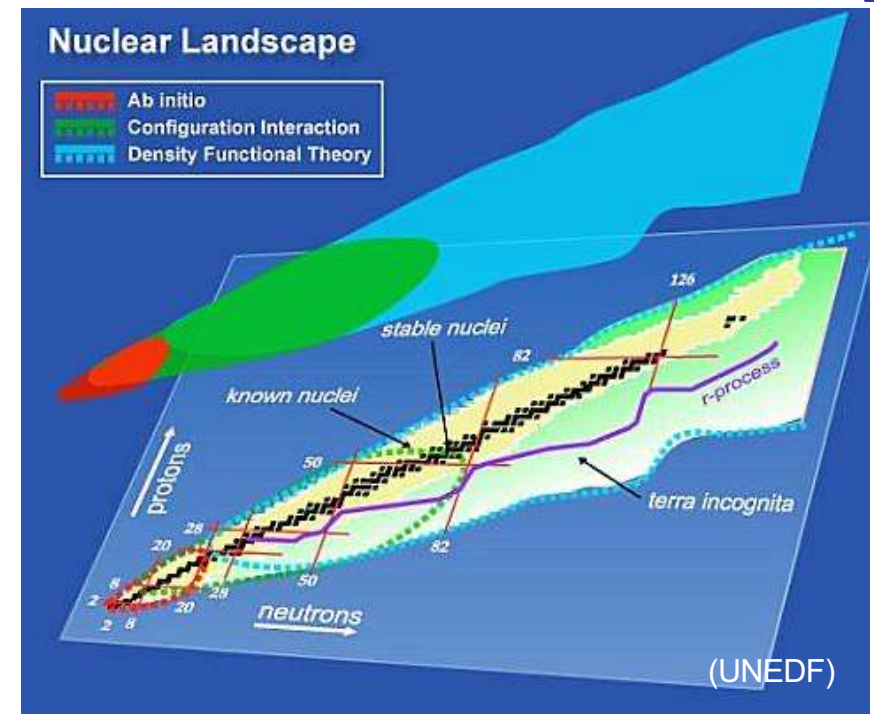
- static and dynamic properties of finite nuclei across the nuclide map (nuclear masses, excitations,...)
- nuclear processes and reactions (beta decays, beta delayed neutron emission, neutron capture, neutrino-induced reactions, nuclear fission ...)
- equation of state of nuclear matter

- **Nonrelativistic**

- Skyrme functionals
- Gogny functionals
- ...

- **Relativistic**

- finite range meson exchange functionals
- point coupling functionals
- density dependent functionals
- ...



# THE ORIGIN OF NUCLEAR MAGNETISM

**Orbital magnetic moment** from from orbiting charged particles

- proportional to orbital angular momentum

$$\vec{\mu}_i^l = g_l(i) \vec{l}_i$$

$$g_l(p) = 1 \mu_N$$

$$g_l(n) = 0$$

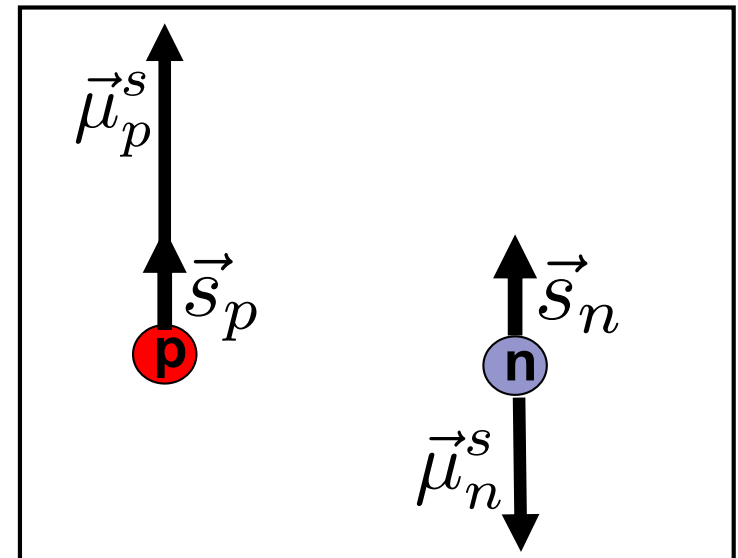
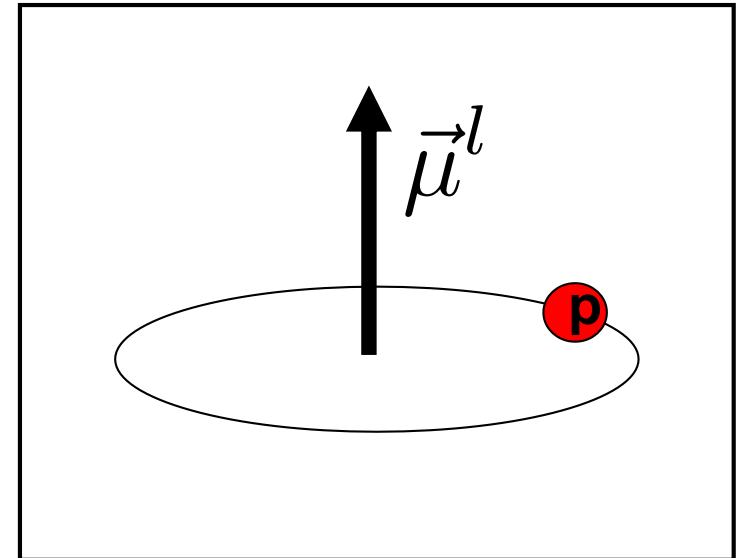
**Spin magnetic moment** from the intrinsic spin nucleons

- proportional to intrinsic spin

$$\vec{\mu}_i = g_s(i) \vec{s}_i$$

gyromagnetic factors (free nucleons)

$$g_s(i) = \begin{aligned} g_p &= 2 \mu_p = 5.585695 \mu_N \\ g_n &= 2 \mu_n = -3.826085 \mu_N \end{aligned}$$



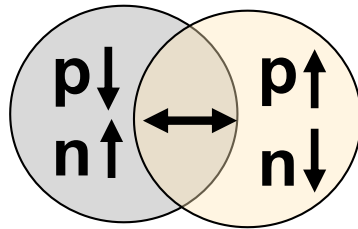
# MAGNETIC DIPOLE TRANSITIONS

## Isovector M1 spin-flip transitions

- induced by  $\sigma T_3$  operator

$$\Delta J=1, \Delta L=0, \Delta \pi=0, \Delta S=1, \Delta T=1$$

$$J^\pi=0^+(\text{GS}) \rightarrow J^\pi=1^+$$

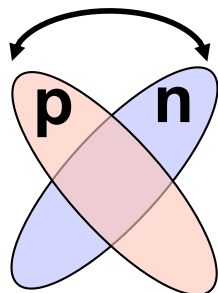


- Transitions between spin-orbit partner states allowed

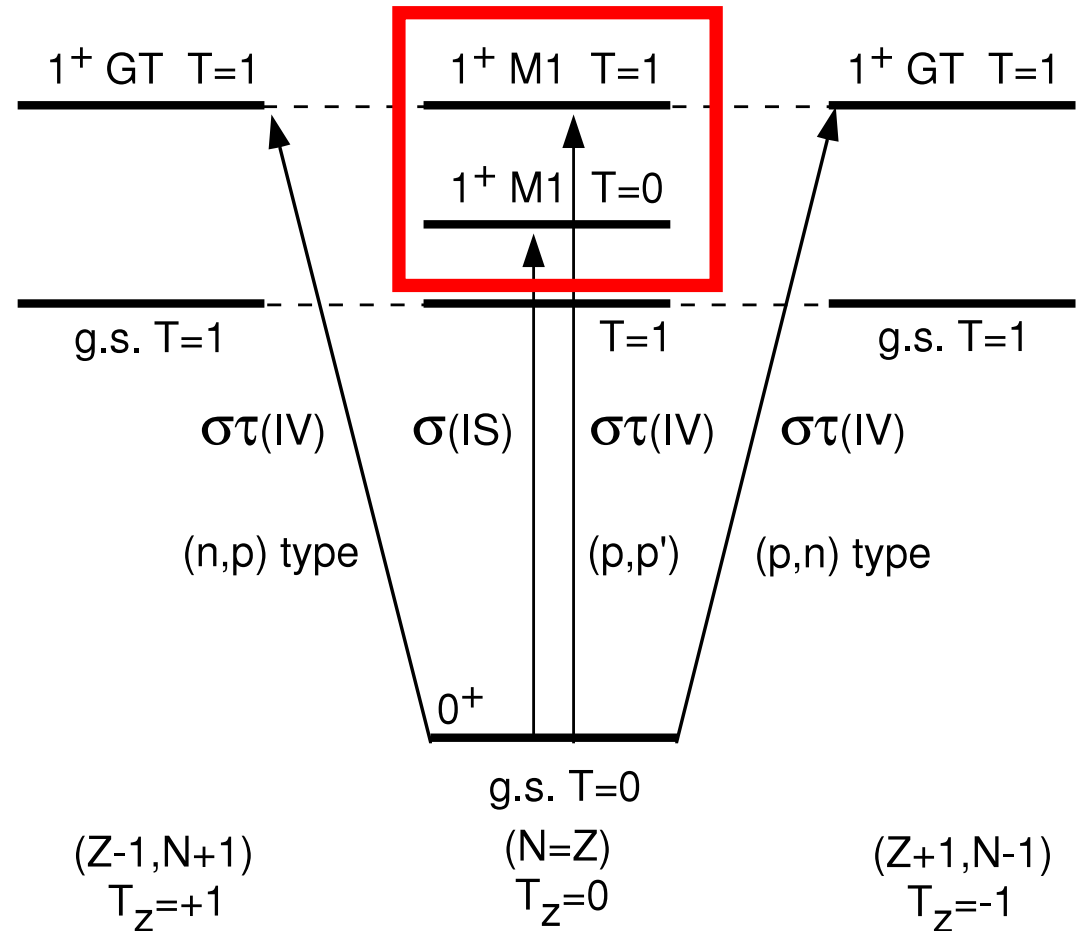
M1 transitions can also be induced by the orbital angular momentum operator  $\vec{l}$

**Scissors mode** (orbital M1,  $\Delta T=1$ )

K. Heyde et al., RMP 82, 2374 (2010).



Y. Fujita et al., PNP 66, 549–606 (2011).



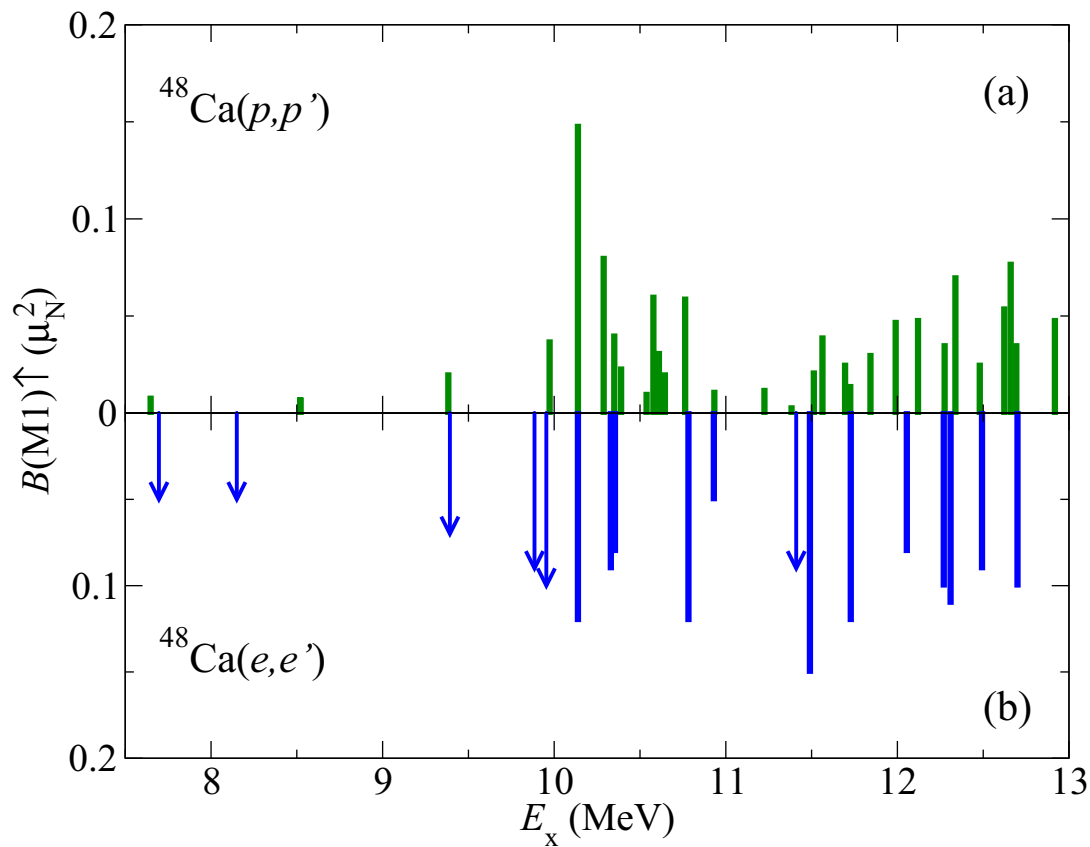
Isovector M1 spin-flip excited states are analogous to Gamow-Teller states in neighboring nuclei

## Why are M1 transitions important?

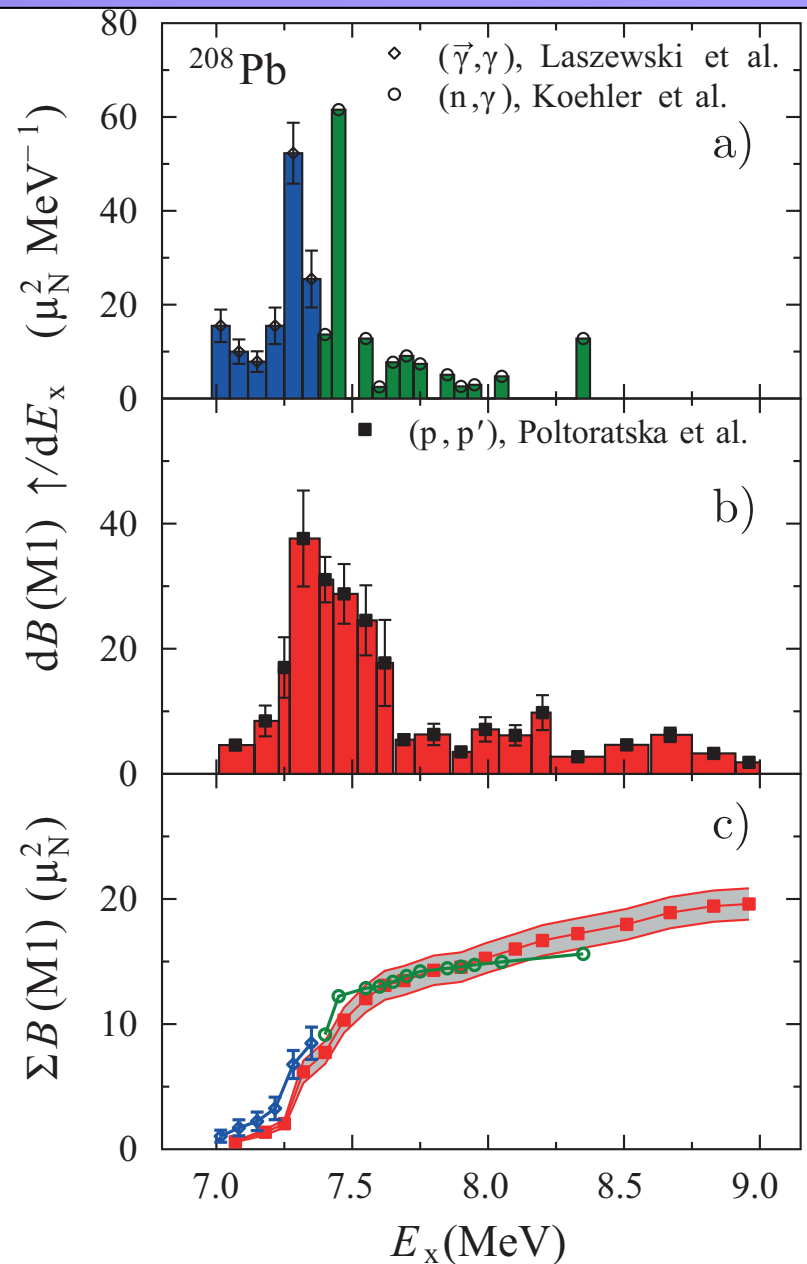
- Since they include transitions between spin-orbit partner states, M1 transitions are important for the understanding of single-particle properties, spin-orbit interaction and shell closures from stable toward exotic nuclei
- IV M1 transitions can probe the inelastic neutrino-nucleus reactions of relevance for neutrino physics and astrophysics (supernovae, etc.)
- M1 response can be used to resolve the problem of quenching of spin-isospin response nuclei, necessary for the description of double  $\beta$ -decay matrix elements
- M1 transitions can affect the radiative neutron capture cross sections – nuclear astrophysics applications require large-scale calculations of M1 response
- ❖ Skyrme functionals which successfully describe electric transitions, have difficulties to reproduce the experimental data on magnetic transitions. Calculations with Gogny force required additional factor of 2 for the M1 transition strengths. More theoretical and experimental studies are needed.

# MAGNETIC DIPOLE (M1) TRANSITIONS IN NUCLEI

Magnetic dipole (M1) transitions in magic nuclei  $^{48}\text{Ca}$  and  $^{208}\text{Pb}$  from recent experimental studies



M. Mathy et al., PRC 95, 054316 (2017).



J. Birkhan et al., PRC 94, 041302(R) (2016).

# RELATIVISTIC NUCLEAR ENERGY DENSITY FUNCTIONAL

- Relativistic point coupling model



- The basis is an effective Lagrangian with four-fermion (contact) interaction terms; isoscalar-scalar, isoscalar-vector, isovector-vector, derivative term

$$\begin{aligned}
 \mathcal{L} = & \bar{\psi}(i\gamma \cdot \partial - m)\psi \\
 & - \frac{1}{2}\alpha_S(\hat{\rho})(\bar{\psi}\psi)(\bar{\psi}\psi) - \frac{1}{2}\alpha_V(\hat{\rho})(\bar{\psi}\gamma^\mu\psi)(\bar{\psi}\gamma_\mu\psi) \\
 & - \frac{1}{2}\alpha_{TV}(\hat{\rho})(\bar{\psi}\vec{\tau}\gamma^\mu\psi)(\bar{\psi}\vec{\tau}\gamma_\mu\psi) \\
 & - \frac{1}{2}\delta_S(\partial_\nu\bar{\psi}\psi)(\partial^\nu\bar{\psi}\psi) - e\bar{\psi}\gamma \cdot A\frac{(1-\tau_3)}{2}\psi
 \end{aligned}$$

- many-body correlations encoded in density-dependent coupling functions that are motivated by microscopic calculations but parameterized in a phenomenological way
- Extensions: pairing correlations in finite nuclei [T. Niksic, et al., Comp. Phys. Comm. 185, 1808 \(2014\).](#)
  - Relativistic Hartree-Bogoliubov model (e.g. with Gogny or separable form of the pairing interaction [Y. Tian et al., PLB 676, 44 \(2009\).](#))

# MAGNETIC DIPOLE (M1) TRANSITION OPERATORS

## ➤ M1 transition operator – spin and orbital angular momentum operators

$$\hat{\mu}_{1\nu} = \sum_{k=1}^A \begin{pmatrix} \hat{\mu}_{1\nu}^{(IS)}(11)_k & 0 \\ 0 & \hat{\mu}_{1\nu}^{(IS)}(22)_k \end{pmatrix} \otimes 1_\tau - \sum_{k=1}^A \begin{pmatrix} \hat{\mu}_{1\nu}^{(IV)}(11)_k & 0 \\ 0 & \hat{\mu}_{1\nu}^{(IV)}(22)_k \end{pmatrix} \otimes \hat{\tau}_3$$

$$\hat{\mu}_{1\nu}^{(IS,IV)}(11)_k = \hat{\mu}_{1\nu}^{(IS,IV)}(22)_k = \frac{\mu_N}{\hbar} (g_\ell^{IS,IV} \hat{\ell}_k + g_s^{IS,IV} \hat{s}_k) \cdot \nabla (r Y_{1\nu}(\Omega_k))$$

## ➤ Gyromagnetic factors

- orbital  $g_\ell^\pi = 1$   $g_\ell^\nu = 0$
- spin  $g_s^{\pi(\nu)} = 5.586$  ( $-3.826$ )

- isoscalar  $g_\ell^{IS} = \frac{g_\ell^\pi + g_\ell^\nu}{2} = 0.5$

- isovector  $g_\ell^{IV} = \frac{g_\ell^\pi - g_\ell^\nu}{2} = 0.5$

$$g_s^{IS} = \frac{g_s^\pi + g_s^\nu}{2} = 0.880$$

$$g_s^{IV} = \frac{g_s^\pi - g_s^\nu}{2} = 4.706$$

Largest factor



# M1 TRANSITION STRENGTH DISTRIBUTIONS

- Relativistic Quasiparticle Random Phase Approximation (RQRPA) equations

$$\begin{pmatrix} A^J & B^J \\ B^{*J} & A^{*J} \end{pmatrix} \begin{pmatrix} X^{\nu, JM} \\ Y^{\nu, JM} \end{pmatrix} = \hbar\omega_\nu \begin{pmatrix} 1 & 0 \\ 0 & -1 \end{pmatrix} \begin{pmatrix} X^{\nu, JM} \\ Y^{\nu, JM} \end{pmatrix}$$

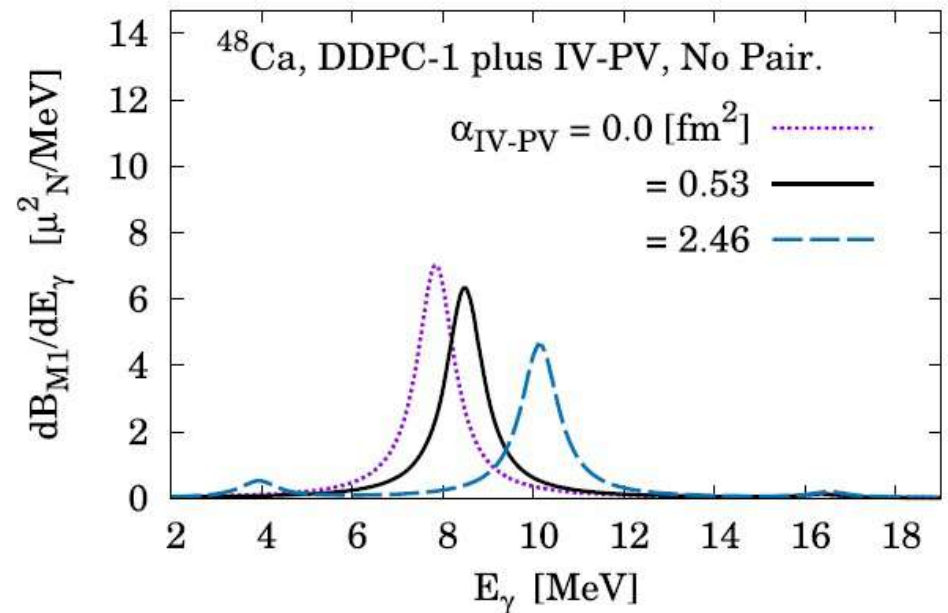
- Includes also contribution from the pseudovector interaction term to describe unnatural parity transitions  $J^\pi=1^+$

$$\mathcal{L}_{IV-PV} = -\frac{1}{2} \alpha_{IV-PV} [\bar{\Psi}_N \gamma^5 \gamma^\mu \vec{\tau} \Psi_N] \cdot [\bar{\Psi}_N \gamma^5 \gamma_\mu \vec{\tau} \Psi_N]$$

- The PV coupling strength is constrained by exp. M1 energies in  $^{48}\text{Ca}$  and  $^{208}\text{Pb}$

## Transition strength

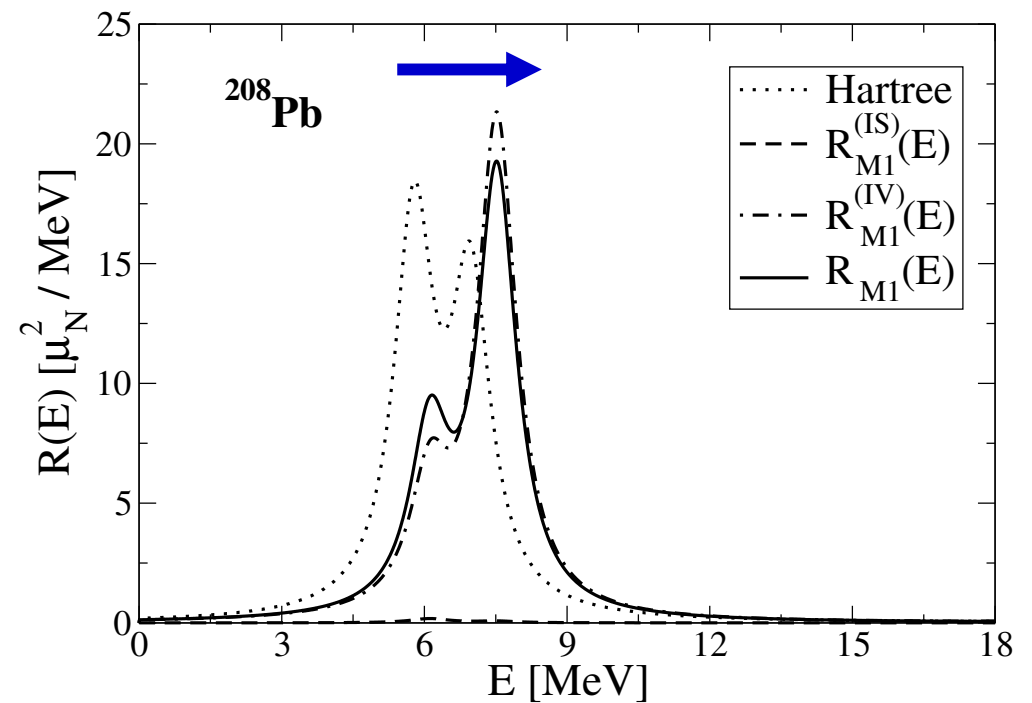
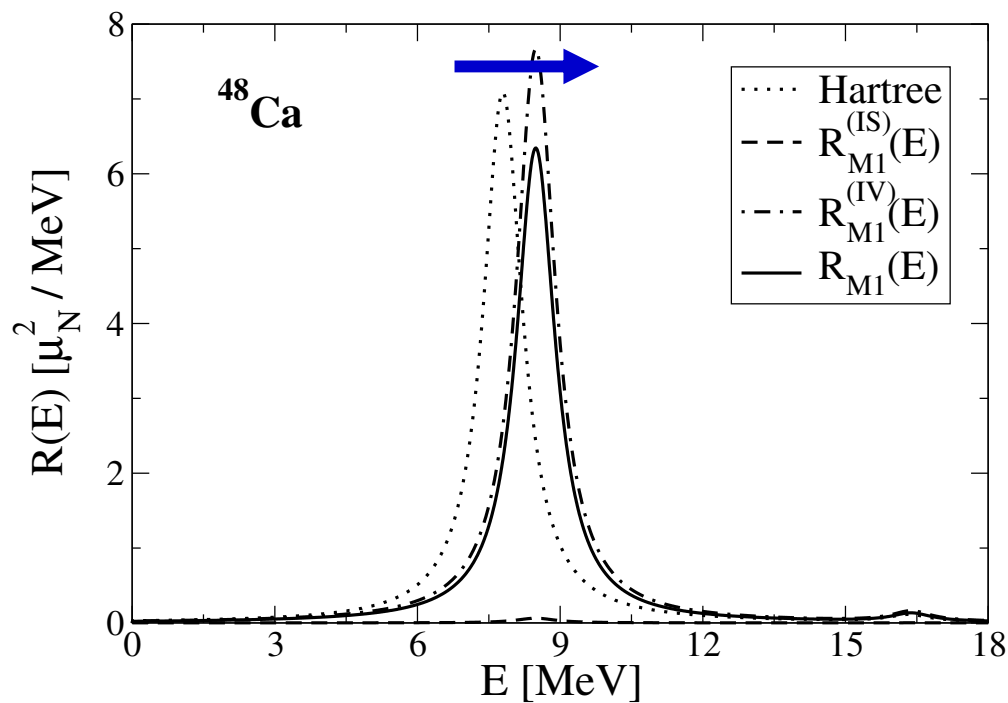
$$B(MJ, \omega_\nu) = \left| \sum_{\kappa\kappa'} \left( X_{\kappa\kappa'}^{\nu, J0} \langle \kappa || \hat{\mu}_J || \kappa' \rangle + (-1)^{j_\kappa - j_{\kappa'} + J} Y_{\kappa\kappa'}^{\nu, J0} \langle \kappa' || \hat{\mu}_J || \kappa \rangle \right) \times \left( u_\kappa v_{\kappa'} + (-1)^J v_\kappa u_{\kappa'} \right) \right|^2$$



# M1 TRANSITION STRENGTH DISTRIBUTIONS

## M1 transition strength for $^{48}\text{Ca}$ and $^{208}\text{Pb}$ :

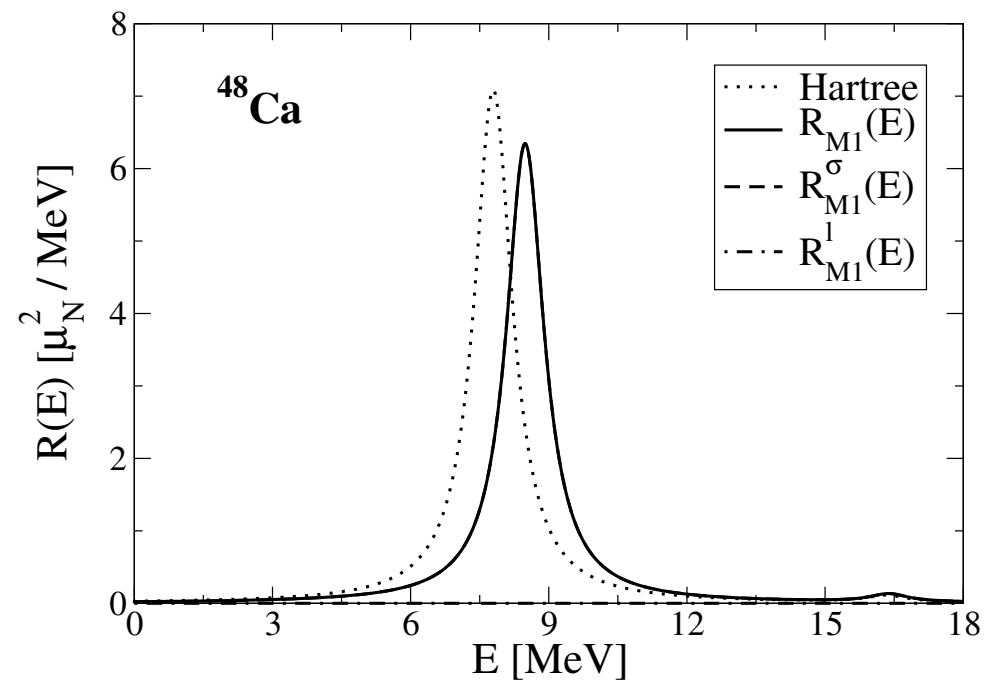
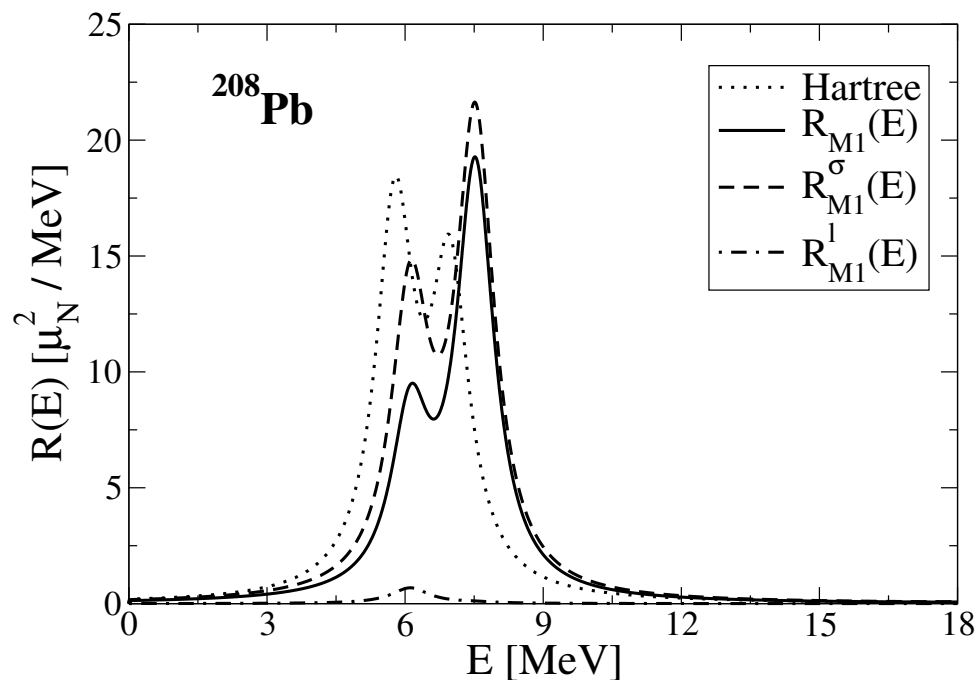
- unperturbed Hartree response
- isoscalar response (small)
- isovector response (large)
- total response (dominated by the isovector response, moved toward higher energies above Hartree response)



# M1 TRANSITION STRENGTH DISTRIBUTIONS

## M1 transition strength for $^{48}\text{Ca}$ and $^{208}\text{Pb}$ :

- unperturbed Hartree response
- spin response (large)
- orbital response (small)
- total response (dominated by the spin response)



## Pairing effects on M1 transitions

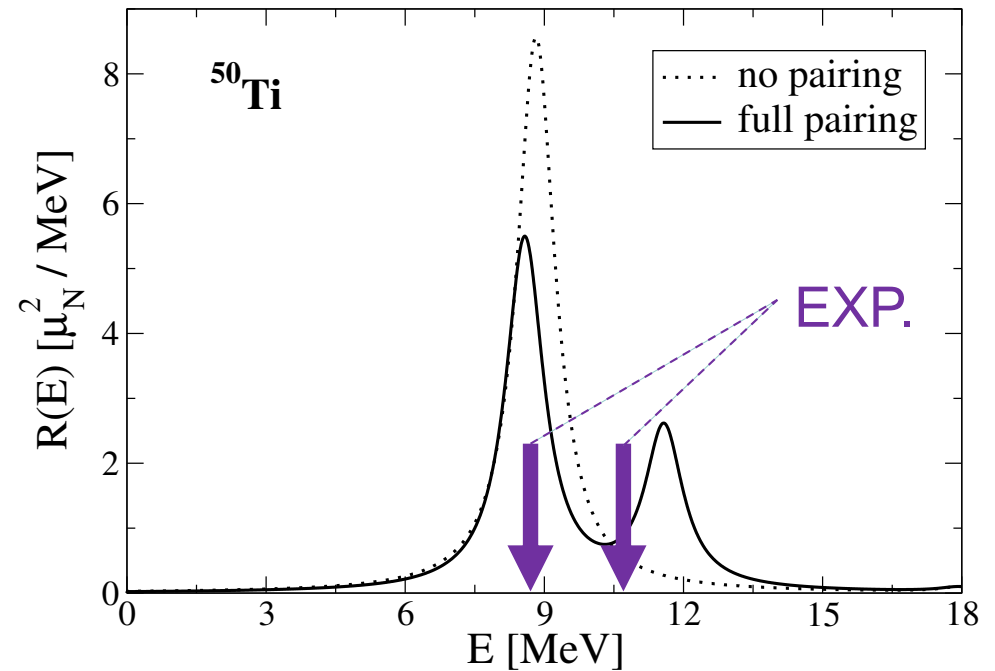
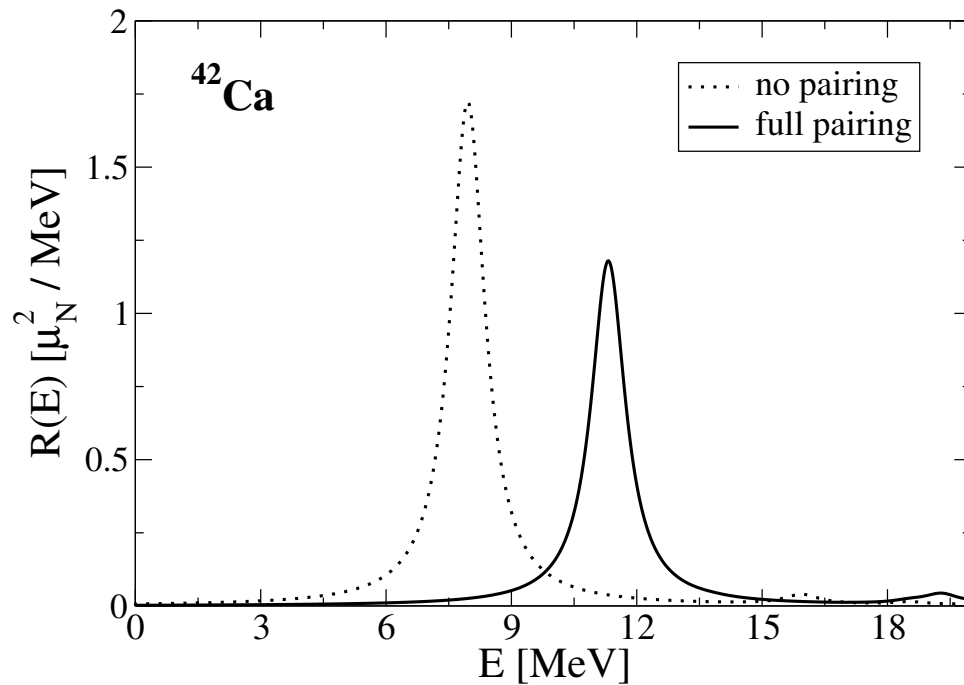
**$^{42}\text{Ca}$** : single excitation peak at 11.3 MeV, dominated by the transition

$$(\nu 1 f_{7/2}^{-1} \rightarrow \nu 1 f_{5/2})$$

**$^{50}\text{Ti}$** : pairing interaction causes the splitting of M1 response, necessary to reproduce exp. data. Two main transitions:

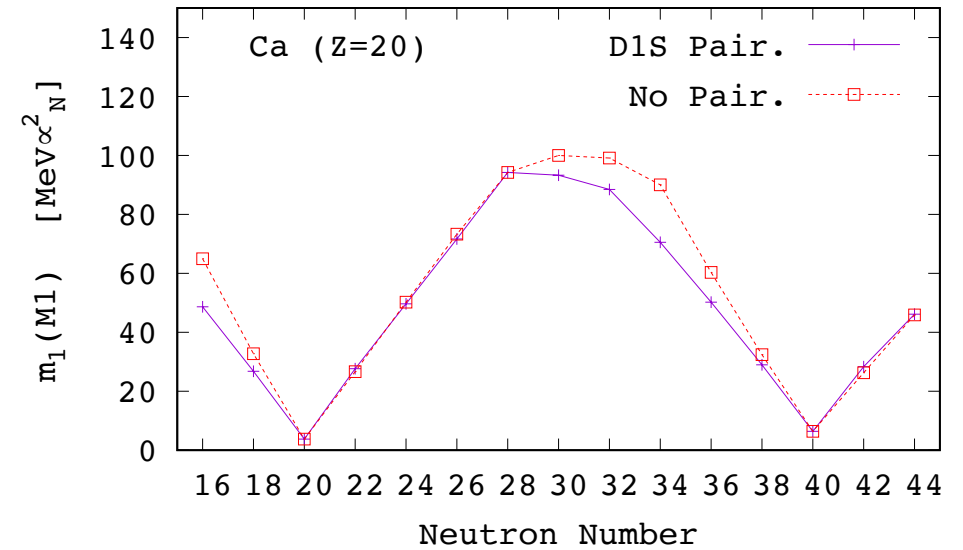
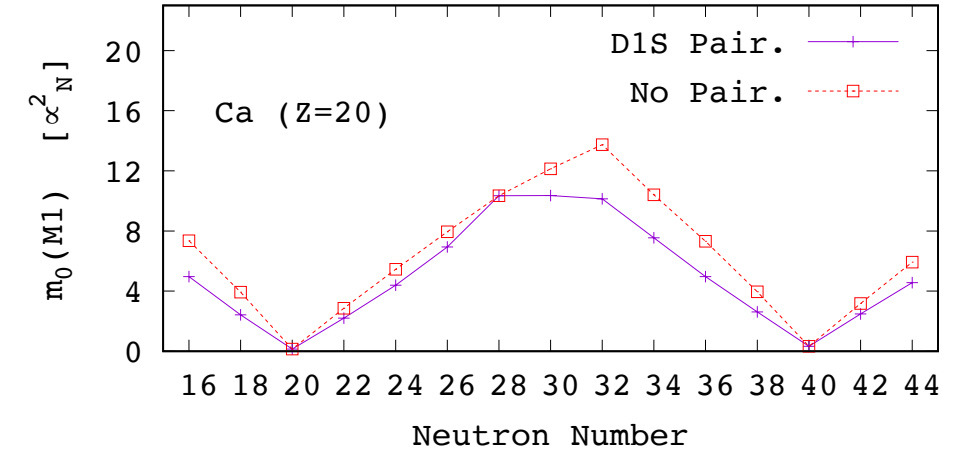
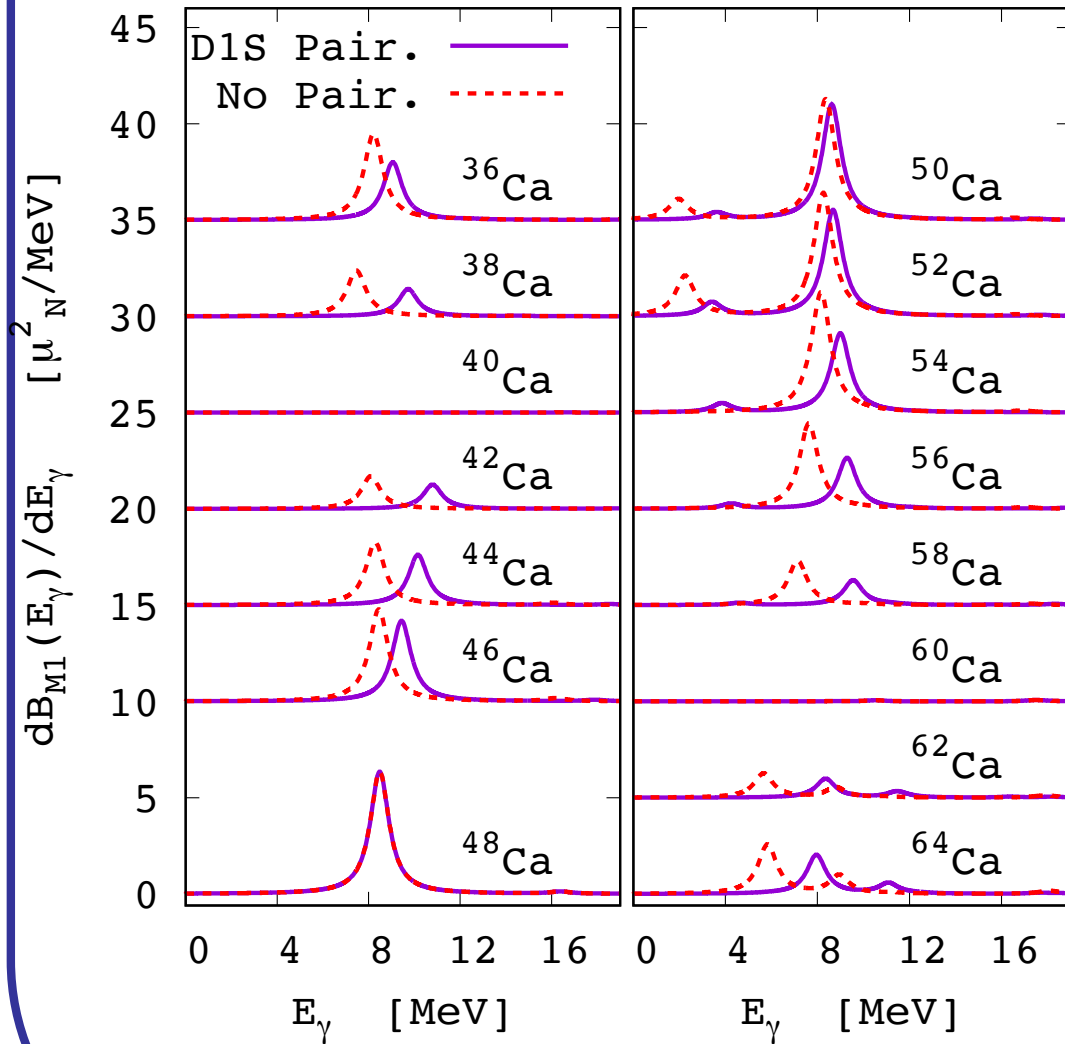
$$(\pi 1 f_{7/2}^{-1} \rightarrow \pi 1 f_{5/2})$$

$$(\nu 1 f_{7/2}^{-1} \rightarrow \nu 1 f_{5/2})$$



Exp. data = D. I. Sober et al., PRC 31, 2054 (1985).

- The evolution of M1 transition strength distributions for Ca isotopes



- For open-shell nuclei, the pairing interaction affects the M1 excitations.

## Why are $^{40}\text{Ca}$ and $^{60}\text{Ca}$ M1 "silent" nuclei ?

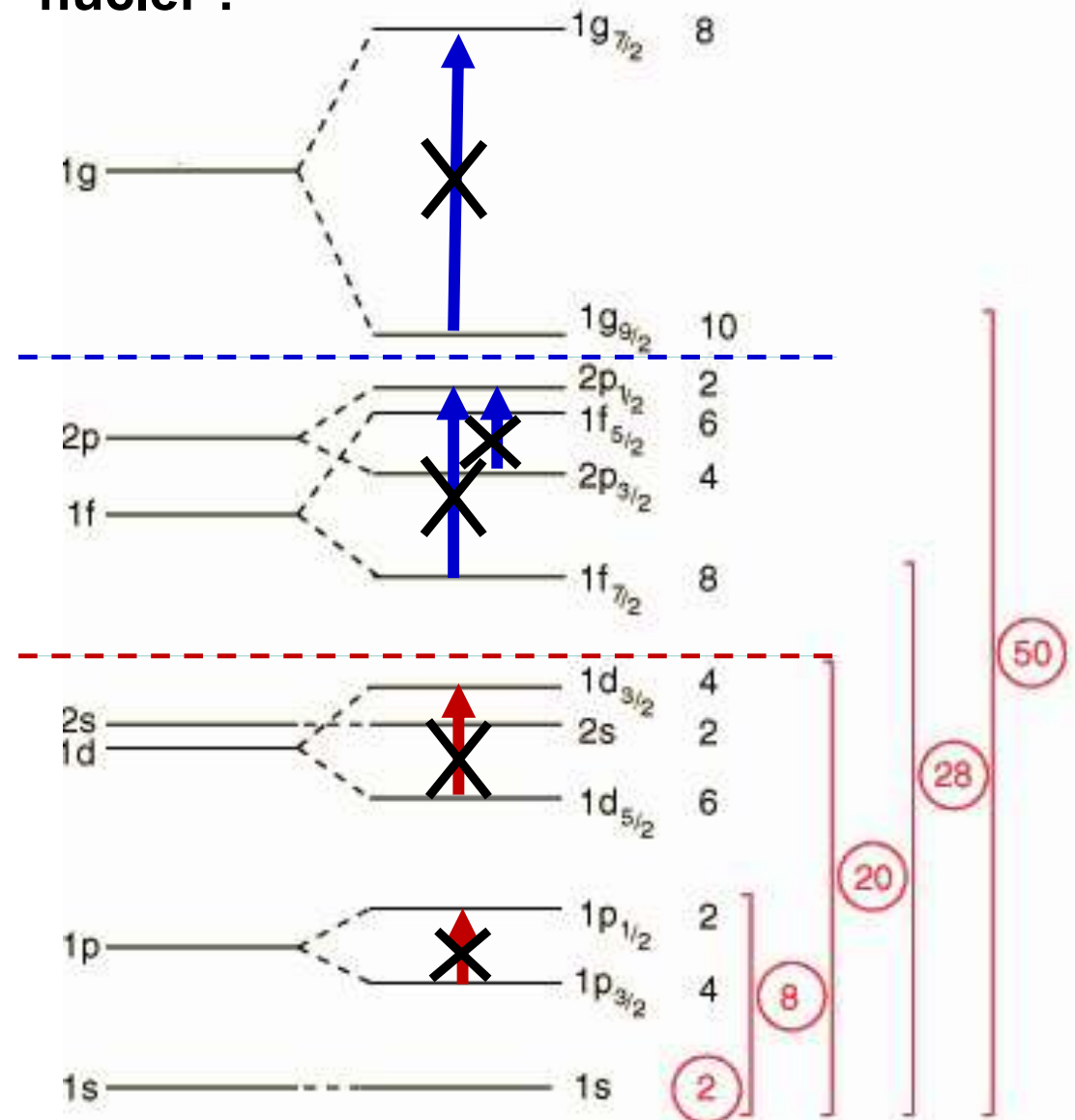
M1 transitions are composed from transitions between spin-orbit partner states

$^{40}\text{Ca}$  ( $Z=N=20$ )

$^{60}\text{Ca}$  ( $Z=20, N=40$ )

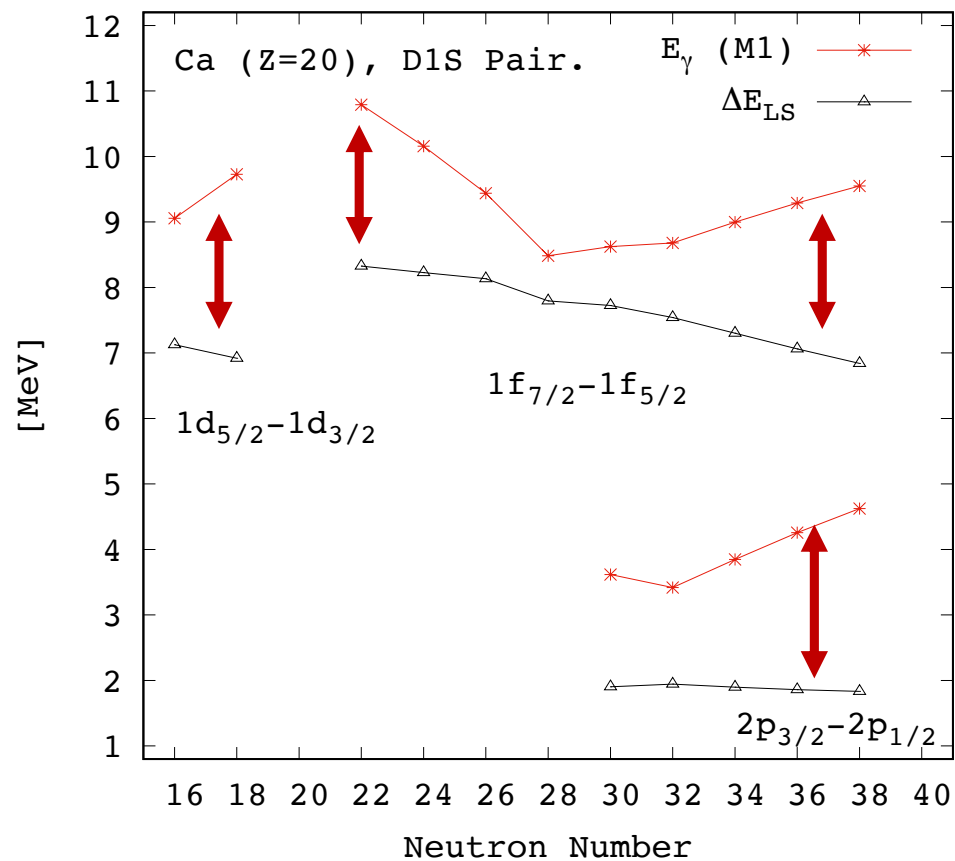
All spin-orbit states below Fermi level are fully occupied, and above Fermi level empty

No particle-hole transitions between spin-orbit partners possible  
 $\Rightarrow$  M1 transitions are forbidden

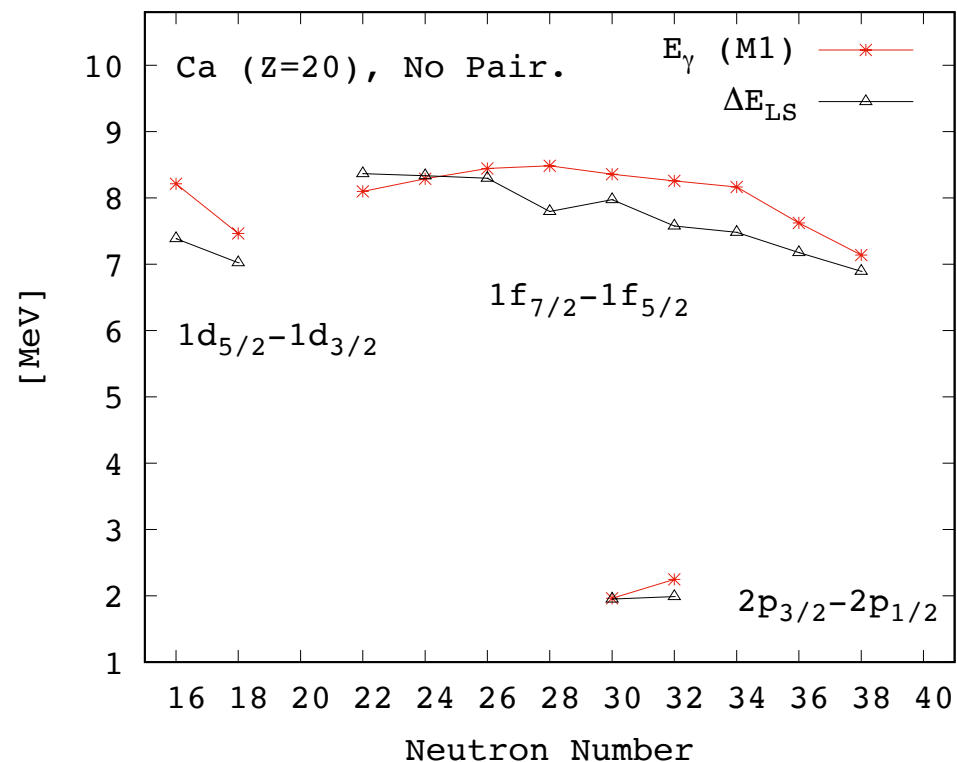


# Spin-orbit splitting energies vs. M1 excitation energies

## Complete QRPA calculation

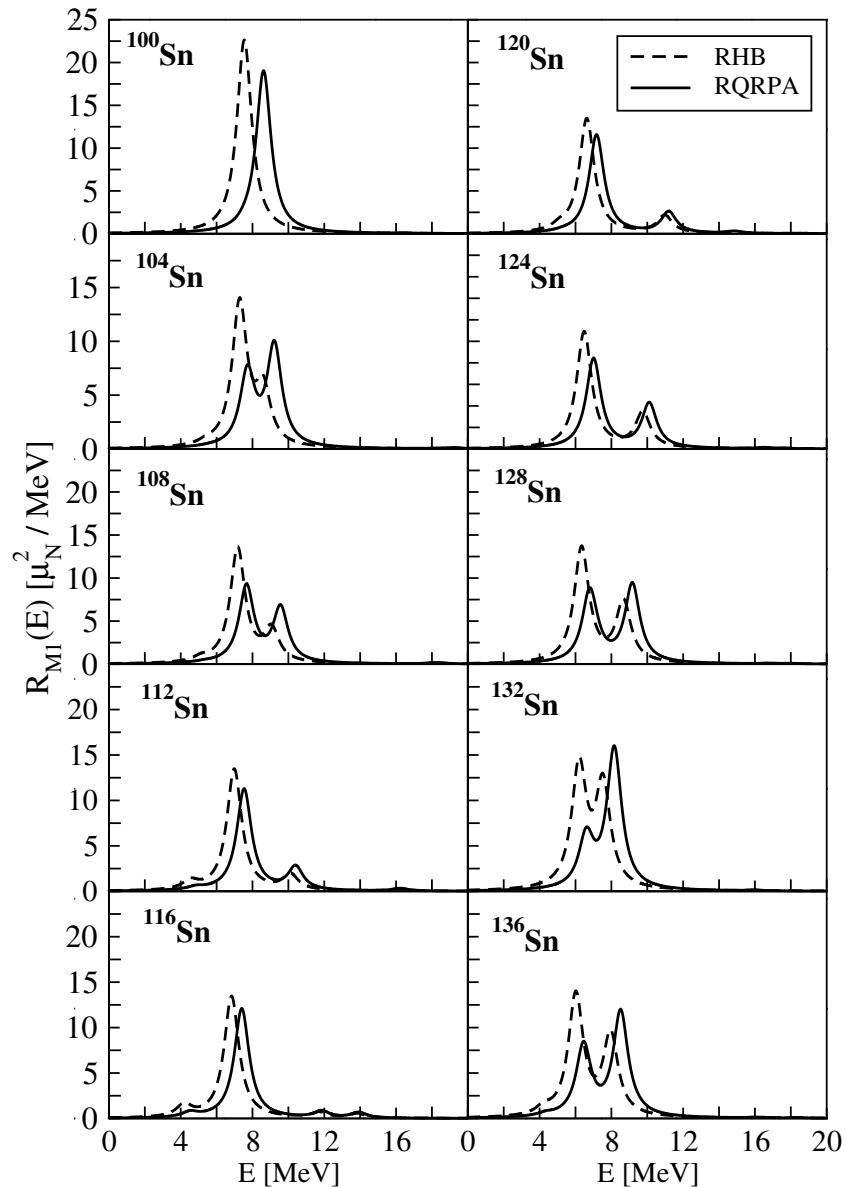


## Without pairing interaction

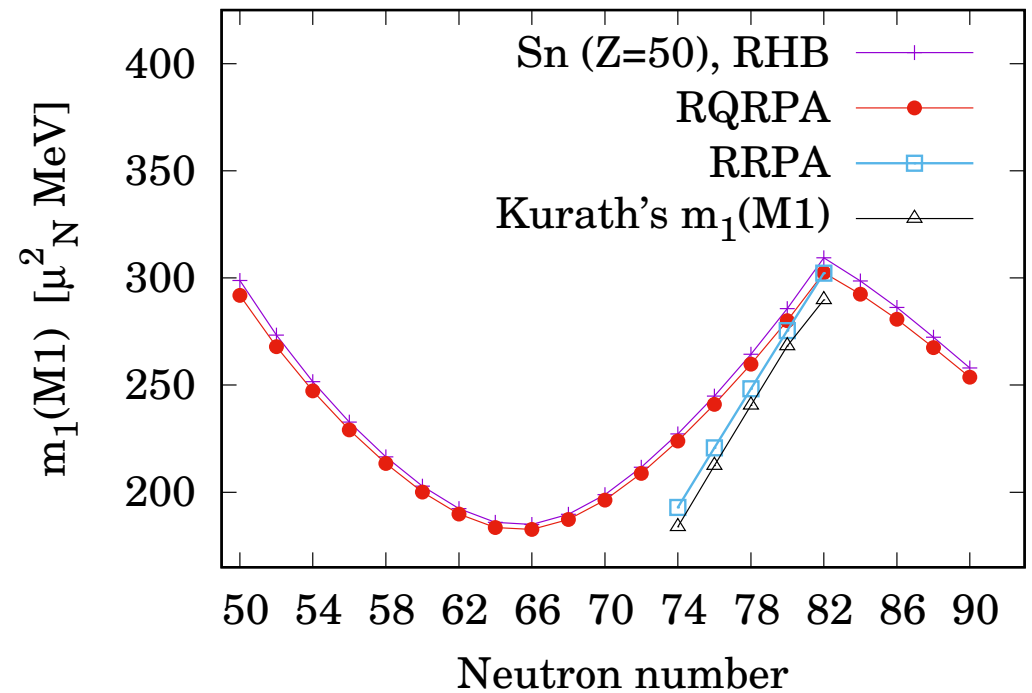


The differences between spin-orbit splittings and M1 excitation energies demonstrate the role of the (residual) interactions

# M1 transitions in Sn isotope chain – evolution toward neutron rich nuclei

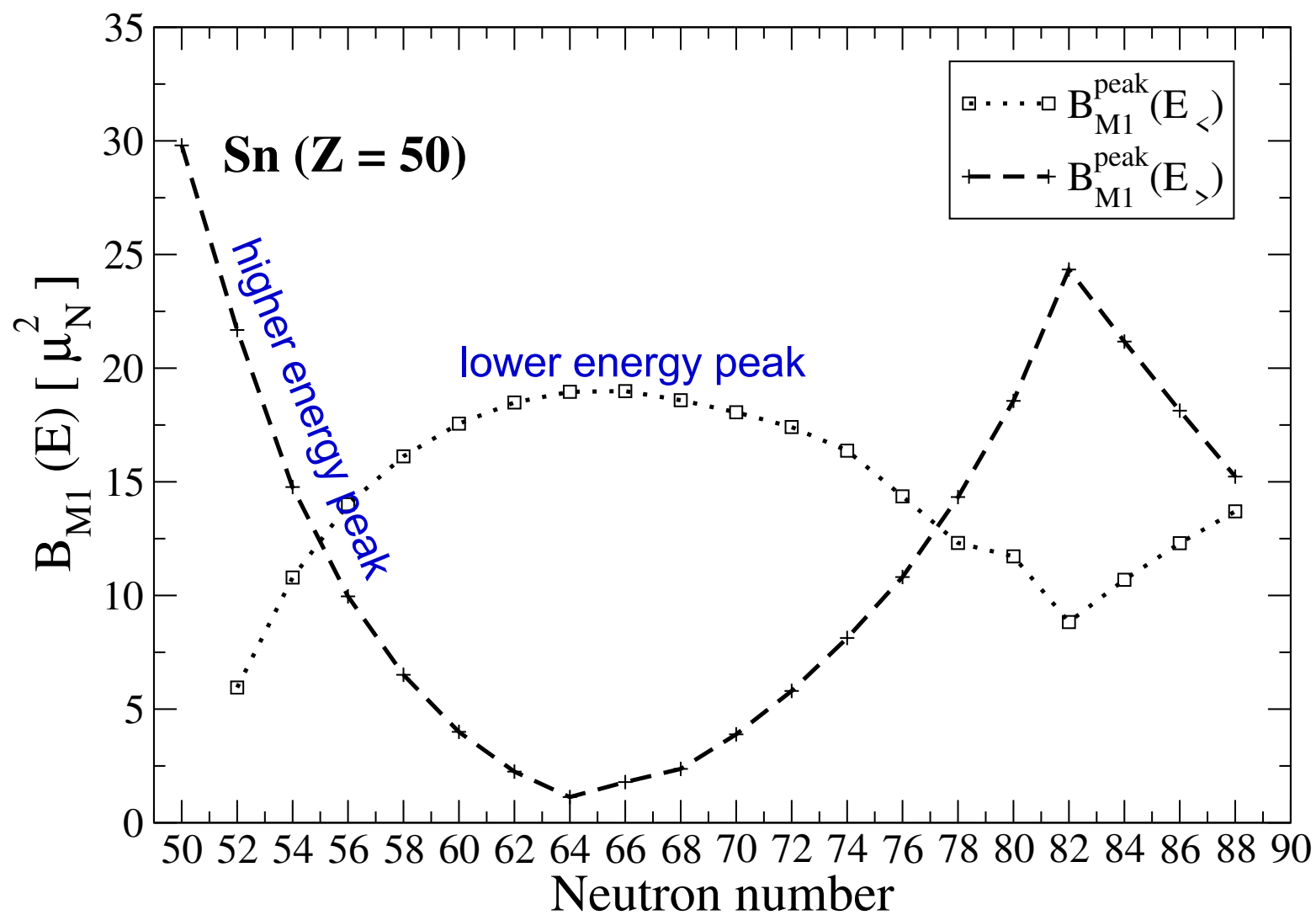


- Energy weighted M1 transition strength, compared with the Kurath's sum rule values

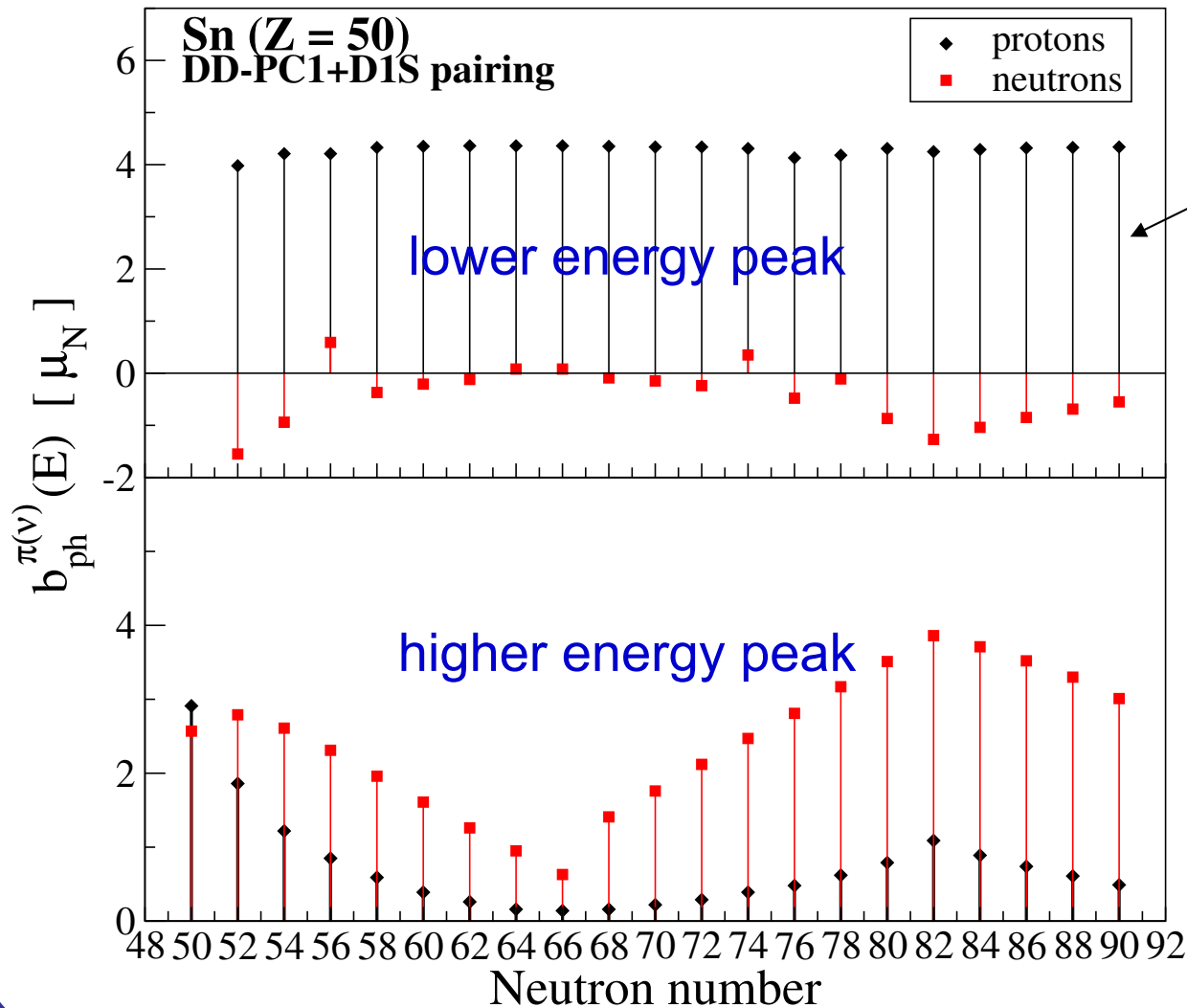




The interplay of the transition strength of the two main M1 peaks along Sn isotope chain



## Partial M1 transition strengths for relevant 2qp configurations



relevant contributions come from proton transitions  
 $(\pi 1g_{9/2} \rightarrow \pi 1g_{7/2})$

Neutron transitions

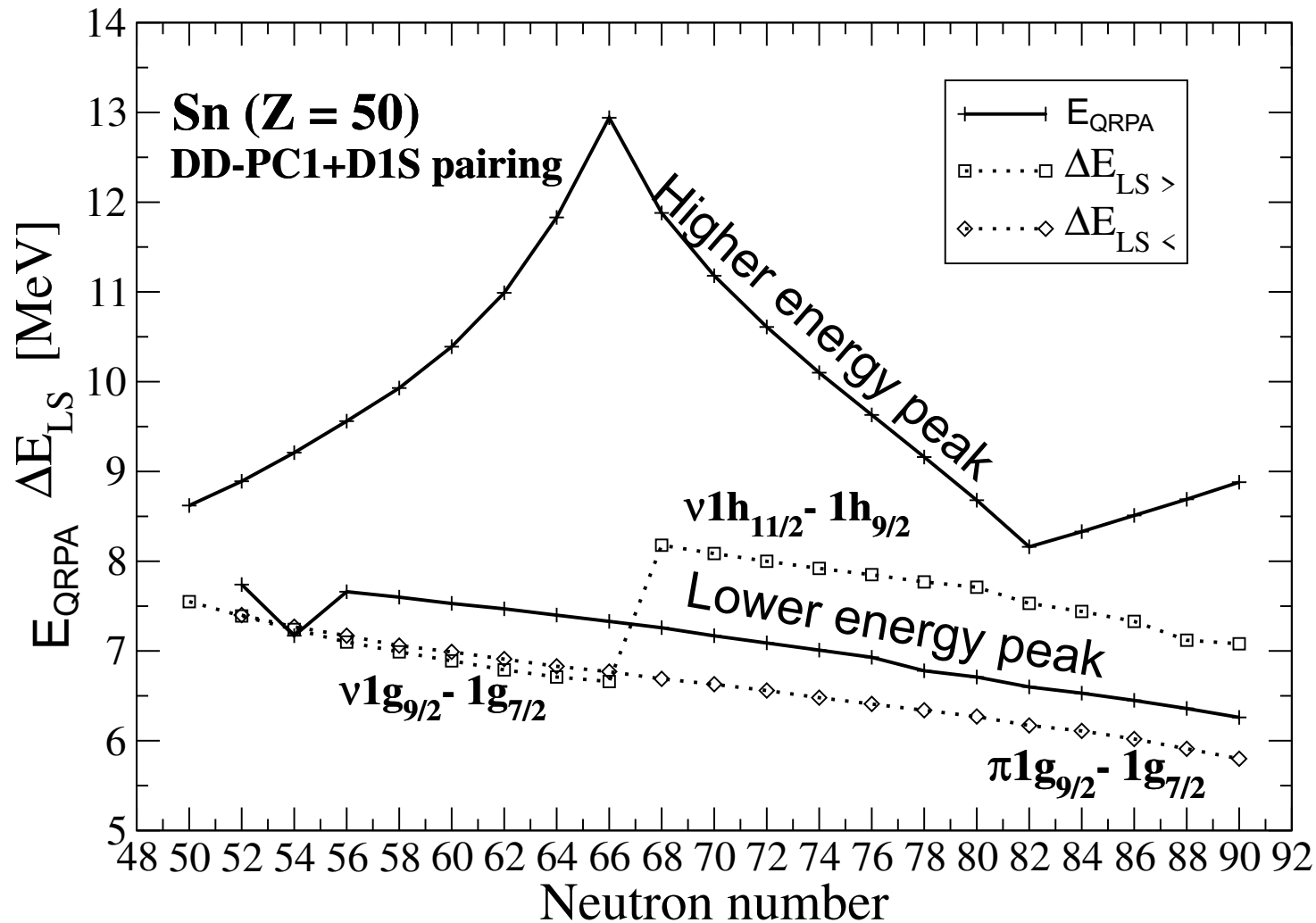
$^{104-116}\text{Sn}$ :  
 $(\nu 1g_{9/2} \rightarrow \nu 1g_{7/2})$   
 $(\nu 2d_{5/2} \rightarrow \nu 2d_{3/2})$

$^{116}\text{Sn}$ - neutron transition is suppressed because  $\nu 1g_{7/2}$  becomes occupied

$^{118-140}\text{Sn}$

$(\nu 1h_{11/2} \rightarrow \nu 1h_{9/2})$

Comparison of the M1 excitation energies with relevant spin-orbit splittings  
 - Demonstrate important role of the QRPA residual interaction for M1 transitions



# THE QUENCHING OF $g$ -FACTORS FROM M1 TRANSITIONS

- In general, model calculations provide more M1 transition strength than the experimental data. Often the quenching in  $g$ -factors (0.6-0.75) is introduced in models to resolve this discrepancy.
- The quenching of  $g$ -factors remains an open question to date.

The total RQRPA (DD-PC1) transition strength in comparison to the new experimental data from inelastic proton scattering - [S. Bassauer et al., PRC 102, 034327 \(2020\)](#).

	$\sum B_{M1}^{th.}(\mu_N^2)$	$\sum B_{M1}^{exp.}(\mu_N^2)$	$g_{eff}/g_{free}$
$^{112}\text{Sn}$	22.81	14.7(1.4)	0.80
$^{114}\text{Sn}$	22.61	19.6(1.9)	0.93
$^{116}\text{Sn}$	22.56	15.6(1.3)	0.83
$^{118}\text{Sn}$	22.76	18.4(2.4)	0.89
$^{120}\text{Sn}$	23.34	15.4(1.4)	0.81
$^{124}\text{Sn}$	25.55	19.1(1.7)	0.86

quenching of the  $g$  factors of the free nucleons, needed to reproduce the exp. data on M1 transition strengths.

Less quenching (**0.8-0.93**) is required in comparison to previous studies (0.6-0.75). Some M1 exp. data above neutron threshold may be missing because of limited accuracy  $\Rightarrow$  weaker quenching?

## CONCLUDING REMARKS

- Relativistic nuclear energy density functional with point coupling interaction has been employed in studies of M1 transitions in nuclei
  - Model calculations in Ca and Sn isotope chains demonstrate the interplay between single-particle properties, spin-orbit splittings, and M1 excitation properties
  - Pairing correlations are essential to reproduce the M1 excitation properties in open shell nuclei
  - The comparison of the calculated M1 transition strength with the new exp. data from inelastic proton scattering on Sn isotopes result in quenching **0.8-0.93** of the g-factors, with perspectives to reduce further

Future work: deformation effects, large-scale calculations for nuclear astrophysics, finite temperature effects on M1 transitions

- M1 transitions - possible additional constraint for the effective nuclear interactions used in the studies of nuclear structure and dynamics

Collaboration with: **Goran Kružić, Tomohiro Oishi**

- G. Kružić, T. Oishi, D. Vale, N. Paar, Phys. Rev. C 102, 044315 (2020).
- T. Oishi, G. Kružić, N. Paar, J. Phys. G: Nucl. Part. Phys. 47, 115106 (2020).
- G. Kružić, T. Oishi, N. Paar, Phys. Rev. C, 103, 054306 (2021).
- T. Oishi, G. Kružić, N. Paar, arXiv:2011.04676 (2021).

This work was supported by the QuantiXLie Centre of Excellence, a project co-financed by the Croatian Government and European Union through the European Regional Development Fund - the Competitiveness and Cohesion Operational Program (Grant KK.01.1.1.01.0004).

For more information please visit:  
<http://bela.phy.hr/quantixlie/hr/>  
<https://strukturnifondovi.hr/>

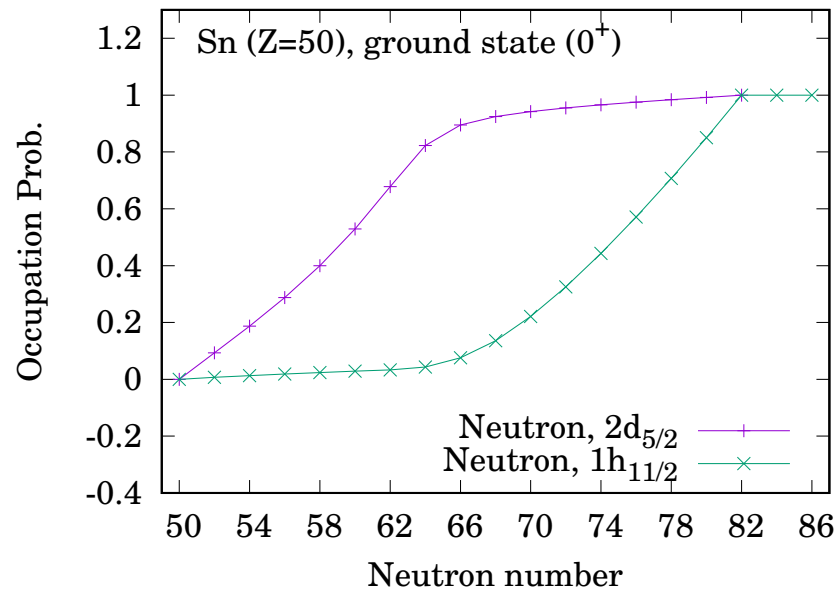
The sole responsibility for the content of this presentation lies with the Faculty of Science, University of Zagreb. It does not necessarily reflect the opinion of the European Union.



Europska unija  
Zajedno do fondova EU



Operativni program  
**KONKURENTNOST  
I KOHEZIJA**



Single-particle occupation probabilities from the RHB model

